A Unified Approach to the Performance Analysis of Speed Estimation Techniques in Mobile Communication

Ali Abdi, *Senior Member, IEEE,* Hong Zhang, *Member, IEEE* and Cihan Tepedelenlioglu, *Member, IEEE*

Abstract

Estimation of the mobile speed, or equivalently, the maximum Doppler frequency, is of importance in a variety of applications in wireless mobile communications. In this paper, a unified framework for the performance analysis of several major speed estimation techniques is presented, which allows a fair comparison between all the methods, analytically. Interestingly, it is proved that all these methods are equivalent, asymptotically, i.e., for large observation intervals. In addition, we have derived closed-from expressions for the bias and variance of a recently proposed covariance-based method. We have also introduced a new estimator which relies on the average number of maxima of the inphase component, and have calculated its variance, analytically. Our extensive performance analysis, supported by Monte Carlo simulations, have revealed that depending on the channel condition and the observation interval, one needs to use a crossing- or a covariance-based technique, to achieve the desired estimation accuracy over a large range of mobile speeds.

Index Terms

This work was presented in part at IEEE Vehicular Technology Conference, Orlando, FL, 2003.

A. Abdi is with the Center for Wireless Communications and Signal Processing Research (CWCSPR), Department of Electrical and Computer Engineering, New Jersey Institute of Technology, Newark, NJ 07012 USA (email: ali.abdi@njit.edu)

H. Zhang was with the CWCSPR, Department of Electrical and Computer Engineering, New Jersey Institute of Technology. He is now with the InterDigital Communications Corporation, King of Prussia, PA 19406, USA (email: hong.zhang@ieee.org)

C. Tepedelenlioglu is with the Department of Electrical Engineering, Arizona State University, Tempe, AZ 85287, USA (email: cihan@asu.edu)

Velocity estimation, Doppler spread, wireless fading channel, speed estimation, performance analysis, asymptotic analysis.

I. INTRODUCTION

Having an accurate estimate of the mobile speed, which provides information about the rate of change of the channel, is essential for handoff, dynamic channel assignment, adaptive transmission, power control, geolocation applications, etc [1]–[4].

There are four major classes of speed estimation techniques in the literature: crossing-based techniques [1], [5], covariance-based methods [4], [6], [7], power spectrum based methods [8], [9], and maximum likelihood (ML) based approaches [3], [10]. Among these speed estimation solutions, crossing-based and covariance-based methods are of low complexity and therefore some of them have been extensively used so far. However, analytic performance analysis of these two approaches, which helps the system designer to choose among different methods without extensive Monte Carlo simulations, is missing.[1] In this paper we consider four crossing-based and two covariance-based schemes, and present a unified theoretical performance analysis framework. In addition, we propose a new crossing-based estimator, relying upon the number of maxima of the inphase component. We also derive a new closed-form expression for a covariance-based method. Performances of the estimators are studied for finite-length observation intervals, as well as large intervals.

The rest of this paper is organized as follows. The channel model is discussed in Section II. In Section III all the six estimators are derived and their bias properties are discussed. Section IV presents the unified performance analysis framework, along with exact variance expressions for the inphase-based methods and some asymptotic results. Simulations of the envelope-based techniques, for which theoretical performance analysis is not tractable, are given in Section V, along with a comprehensive performance comparison of all the methods. Section VI concludes the paper.

[1]For the analytical performance analysis for the power spectrum and ML methods, we refer the readers to [8] and [10], respectively.

II. The Channel Model

In a noisy Rician frequency-flat fading channel, with two-dimensional propagation of planar waves, the lowpass complex envelope at the mobile station (MS), downlink, can be written as

$$z(t) = x(t) + n(t), \tag{1}$$

where the complex Gaussian process $n(t)$ represents the receiver noise, whereas the complex process $x(t)$ includes the random diffuse component and the deterministic line-of-sight (LOS) component [11]

$$x(t) = \sqrt{\frac{\Omega}{K+1}}h(t) + \sqrt{\frac{K\Omega}{K+1}}\exp[j\omega_D \cos(\phi_0)t + \psi_0]. \tag{2}$$

In the above equation, $h(t)$ is the superposition of a large number of multipath components, satisfying the central limit theorem, such that $h(t)$ is a zero-mean unit-power complex Gaussian process, i.e., $E[|h(t)|^2] = 1$. Moreover, $\omega_D = 2\pi f_D = 2\pi v/\lambda = 2\pi v f_c/c$ is the maximum Doppler frequency in rad/sec, v is the MS speed, λ is the wavelength, f_c is the carrier frequency, and c is the speed of light. We also have $j^2 = -1$, and ϕ_0 and ψ_0 stand for the angle-of-arrival (AOA) in the two-dimensional plane and the phase of the LOS component, respectively. In eq. (2), $\Omega = E[|x(t)|^2]$ is the total received power, whereas the Rice factor K is the ratio of the LOS power to the diffuse power of $x(t)$. For the received signal at the base station (BS), uplink, the same equations as (1) and (2) hold [12].

For complete characterization of $h(t)$, we need the corresponding correlation function, $r_h(\tau) = E[h(t)h^*(t+\tau)]$, which is given by

$$r_h(\tau) = \int_{-\pi}^{\pi} p_h(\phi)\exp[-j\omega_D \cos(\phi)\tau]d\phi, \tag{3}$$

where $p_h(\phi)$ is the probability density function (PDF) of the AOA in the two-dimensional plane. For $r_x(\tau) = E[x(t)x^*(t+\tau)]$ we have

$$r_x(\tau) = \frac{\Omega}{K+1}r_h(\tau) + \frac{K\Omega}{K+1}\exp[-j\omega_D \cos(\phi_0)\tau]. \tag{4}$$

For isotropic scattering, i.e., $p_h(\phi) = 1/(2\pi)$, we obtain Clarke's correlation model $r_h(\tau) = J_0(\omega_D\tau)$, with $J_0(.)$ as the zero-order Bessel function of the first kind. However, in the presence of nonisotropic scattering, $p_h(\phi)$ and consequently $r_h(\tau)$ could be very far from the uniform PDF and Clarke's model, respectively. The von Mises PDF has proven to be a flexible model

for the nonuniform distribution of AOA both at the MS and the BS, studied in [12] and [13], respectively

$$p_h(\phi) = \exp[\kappa \cos(\phi - \alpha)]/[2\pi I_0(\kappa)], \;\; \phi \in [-\pi, \pi), \tag{5}$$

where $\alpha \in [-\pi, \pi)$ accounts for the mean direction of AOA of multipath components, $\kappa \geqslant 0$ controls the width of the AOA of multipath components, and $I_0(.)$ is the zero-order modified Bessel function of the first kind. For this AOA distribution, the correlation function at the MS can be shown to be [13]

$$r_h(\tau) = I_0\left(\sqrt{\kappa^2 - \omega_D^2\tau^2 + j2\kappa\omega_D\tau\cos\alpha}\right)/I_0(\kappa). \tag{6}$$

The same result holds for the BS [12].

III. Speed Estimation: A Continuous-Time Approach

In this section we adopt the basic propagation mechanism of isotropic scattering with no LOS in a noise-free environment, which entails straightforward derivation and performance analysis of a variety of existing and new speed estimation techniques under the same umbrella. The effect of nonisotropic scattering, LOS, and Gaussian noise will be studied later, either via analytic methods or simulation.

In the absence of noise and LOS, $K = 0$, and assuming $\Omega = 1$, unit received power, one gets $z(t) = x(t) = h(t)$ for the received signal according to (1) and (2). So, in this section we just concentrate on $h(t)$. In what follows and with $r_h(\tau) = J_0(\omega_D\tau)$, we consider two classes of estimation methods: crossing-based and covariance-based techniques. Since the vehicle speed v is proportional to the maximum Doppler frequency ω_D, in the rest of the paper we focus on the estimation of ω_D, to simplify the notation. We may use either $\xi(t) = \Re\{h(t)\}$, the inphase component, where $\Re\{.\}$ gives the real part, or $\eta(t) = |h(t)|^2$, the envelope-squared, each one observed over a time interval of length T. Note that $\xi(t)$ is a zero-mean real Gaussian process with variance $1/2$, whereas $\eta(t)$ has an exponential distribution, i.e., $p(\eta) = \exp(-\eta)$. We use $|h(t)|^2$ rather than $|h(t)|$, the envelope, as the correlation function of envelope-squared in some cases of interest can be expressed in simple closed forms [1], required for analytic studies. For $r_\xi(\tau) = E[\xi(t)\xi(t+\tau)]$ we have $r_\xi(\tau) = (1/2)\Re\{r_h(\tau)\}$. On the other hand, for $r_\eta(\tau) = E[\eta(t)\eta(t+\tau)]$, it is shown that $r_\eta(\tau) = 1 + |r_h(\tau)|^2$ [1]. Hence, with $r_h(\tau) = J_0(\omega_D\tau)$, we obtain $r_\xi(\tau) = (1/2)J_0(\omega_D\tau)$ and $r_\eta(\tau) = 1 + J_0^2(\omega_D\tau)$.

Last but not the least, note that rather than working with the sampled version of $h(t)$, i.e., $h[\ell] = h(\ell T_s),\ \ell = 0, 1, 2, ...$, with T_s as the sampling period, we work with the continuous-time process itself, which allows us to derive closed-form results for the variance of the estimators. The effect of sampling, briefly discussed in [14], is negligible as long as T_s is small enough.

A. Crossing-Based Methods

For a given real random process $y(t)$, let us define $N_y(y_{th}, T)$ as the number of times that the process crosses the threshold level y_{th}, with positive slope, over the time interval $(0, T]$. Also let $M_y(T)$ denote the number of maxima of the process $y(t)$ over the time interval $(0, T]$. The number of zero crossing of $\xi(t)$ is given in [1, p. 66] as

$$E[N_\xi(0, T)] = T\omega_D/(2\pi\sqrt{2}). \tag{7}$$

According to Appendix I, the number of maxima of $\xi(t)$ can be easily derived from (45) as

$$E[M_\xi(T)] = T\omega_D\sqrt{3}/(4\pi). \tag{8}$$

On the other hand, for the level crossing and the maxima of $\eta(t)$, one can obtain the following results from [1, p. 64] and [15, eq. (22)], respectively

$$E[N_\eta(1, T)] = T\omega_D/(e\sqrt{2\pi}), \tag{9}$$

$$E[M_\eta(T)] = T\omega_D 3/(4\pi), \tag{10}$$

where $e = 2.7813$ is the base of the natural logarithm. Based on (7)-(10), the following estimators can be considered

$$\hat{\omega}_{D,1} = (2\pi\sqrt{2})N_\xi(0, T)T^{-1}, \tag{11}$$

$$\hat{\omega}_{D,2} = (4\pi/\sqrt{3})M_\xi(T)T^{-1}, \tag{12}$$

$$\hat{\omega}_{D,3} = (e\sqrt{2\pi})N_\eta(1, T)T^{-1}, \tag{13}$$

$$\hat{\omega}_{D,4} = (4\pi/3)M_\eta(T)T^{-1}. \tag{14}$$

All these four estimators are unbiased, i.e., $E[\hat{\omega}_{D,i}] = \omega_D$, $i = 1, ..., 4$. According to the literature survey of [11] and among these four crossing-based estimators, $\hat{\omega}_{D,2}$ which employs the number of maxima of the inphase component appears to be new.

B. Covariance-Based Methods

1) Covariance matching method: Based on the covariance function definitions $c_\xi(\tau) = r_\xi(\tau) - \{E[\xi(t)]\}^2$ and $c_\eta(\tau) = r_\eta(\tau) - \{E[\eta(t)]\}^2$, along with $r_\xi(\tau) = (1/2)J_0(\omega_D\tau)$, $r_\eta(\tau) = 1 + J_0^2(\omega_D\tau)$, $E[\xi(t)] = 0$, and $E[\eta(t)] = 1$, one obtains

$$c_\xi(\tau) = (1/2)J_0(\omega_D\tau), \tag{15}$$

$$c_\eta(\tau) = J_0^2(\omega_D\tau). \tag{16}$$

According to Taylor expansion we have $J_0(\omega_D\tau) = 1 - (\omega_D^2/4)\tau^2 + O(\tau^4)$, as $\tau \to 0$, where $f_1(t) = O(f_2(t))$ as $t \to 0$ means that $f_1(t)/f_2(t)$ is bounded in a neighborhood around zero. Therefore

$$c_\xi(\tau) = (1/2) - (\omega_D^2/8)\tau^2 + O(\tau^4), \text{ as } \tau \to 0, \tag{17}$$

$$c_\eta(\tau) = 1 - (\omega_D^2/2)\tau^2 + O(\tau^4), \text{ as } \tau \to 0. \tag{18}$$

The quadratic form of the covariance functions in (17) and (18) for small τ, i.e., $c_y(\tau) \approx a - b\omega_D^2\tau^2$, where $a = 1/2, 1$ and $b = 1/8, 1/2$ for $y(t) = \xi(t), \eta(t)$, respectively, motivates to estimate ω_D^2 by fitting a quadratic equation $a - b\omega_D^2\tau^2$ to the sample covariance function, $\hat{c}_y(\tau)$, via a minimum mean squared error (MMSE) procedure, i.e.

$$\min_{\omega_D^2} E\left\{\int_0^{T_0} [\hat{c}_y(\tau) - a + b\omega_D^2\tau^2]^2 d\tau\right\}, \tag{19}$$

where T_0 is sufficiently small. By setting the derivative (with respect to ω_D^2) of the expectation in (19) to zero, the MMSE estimate of ω_D^2 can be shown to be

$$\widehat{\omega_{D,5}^2} = \frac{5a}{3bT_0^2} - \frac{5}{bT_0^5}\int_0^{T_0} \tau^2\hat{c}_y(\tau)d\tau. \tag{20}$$

The natural choice for estimating ω_D from (20) is

$$\hat{\omega}_{D,5} = \sqrt{\widehat{\omega_{D,5}^2}}. \tag{21}$$

Obviously this is a biased estimator for ω_D. To be able to calculate the bias approximately, assume the variance of the estimator is small enough, which allows a first-order Taylor expansion for $\sqrt{\widehat{\omega_{D,5}^2}}$ around $E[\widehat{\omega_{D,5}^2}]$, which implies that $E[\widehat{\omega}_{D,5}] \approx \sqrt{E[\widehat{\omega_{D,5}^2}]}$. This argument is the same as the one used in [14]. With this unbiased estimator

$$\hat{c}_y(\tau) = \frac{1}{T}\int_0^T \left(y(t) - \overline{y(t)}\right)\left(y(t+\tau) - \overline{y(t)}\right) dt, \tag{22}$$

where $\overline{y(t)} = T^{-1}\int_0^T y(t)dt$, we obtain

$$E[\widehat{\omega_{D,5}^2}] = \frac{5a}{3bT_0^2} - \frac{5}{bT_0^5}\int_0^{T_0} \tau^2 c_y(\tau)d\tau. \tag{23}$$

Based on $c_y(\tau) = a - b\omega_D^2\tau^2 + O(\tau^4)$, as $\tau \to 0$, with a and b defined after (17) and (18), eq. (23) can be written as

$$E[\widehat{\omega_{D,5}^2}] = \omega_D^2 + O(T_0^2), \text{ as } T_0 \to 0. \tag{24}$$

Since $\sqrt{1+t} = 1 + O(t)$, as $t \to 0$, we eventually come up the following result for the bias of $\hat{\omega}_{D,5}$, valid for both $\xi(t)$ and $\eta(t)$

$$E[\hat{\omega}_{D,5}] \approx \omega_D + O(T_0^2), \text{ as } T_0 \to 0. \tag{25}$$

Clearly this approximate-asymptotic result, derived analytically, is supposed to provide just an insight into the bias behavior of $\hat{\omega}_{D,5}$ with respect to T_0. The approximation $E[\hat{\omega}_{D,5}] \approx \sqrt{E[\widehat{\omega_{D,5}^2}]}$, with $E[\widehat{\omega_{D,5}^2}]$ given by (23), is useful for any T_0. More conclusions can be made only via Monte Carlo simulation. Also note that for a good-quality estimate of $c_y(\tau)$, T in (22) should be much larger than T_0.

The idea of least-squares fitting of a parabola to the sample covariance function at small lags was first proposed in [6], in a discrete-time setting. However, explicit form of the estimator, such as the one given in (20), the bias analysis discussed in the previous paragraphs and summarized in (23) and (25), and the variance analysis, discussed in the next section, are not addressed in [6]. In the context of spectral moment estimation, closely related to our maximum Doppler estimation problem, utilization of the quadratic form of a correlation function at a *single* small lag, different from the MMSE formulation in (19), is discussed in [16] (see also [17] and [18]). Moreover, the bias/variance analysis of [16] is different from this paper and does not apply to the basic correlation function of interest in wireless communications, i.e., $J_0(\omega_D\tau)$, which is not absolutely integrable. This important issue will be discussed later.

2) Integration method: For an arbitrary real process $y(t)$, we know that $r_{\dot{y}}(\tau) = -r_y''(\tau)$ [7], where dot and prime denote differentiation with respect to the time t and the delay τ, respectively. According to (15) and (16)

$$E[\dot{\xi}^2(t)] = r_{\dot{\xi}}(0) = \omega_D^2/4, \tag{26}$$

$$E[\dot{\eta}^2(t)] = r_{\dot{\eta}}(0) = \omega_D^2. \tag{27}$$

Now based on these two identities, one can consider the following estimator for ω_D^2

$$\widehat{\omega_{D,6}^2} = d\frac{1}{T}\int_0^T \dot{y}^2(t)dt, \tag{28}$$

where $d = 4, 1$ for $y(t) = \xi(t), \eta(t)$, respectively. Note that unlike $\widehat{\omega_{D,5}^2}$ in (20), $\widehat{\omega_{D,6}^2}$ is an unbiased estimator for ω_D^2. However,

$$\hat{\omega}_{D,6} = \sqrt{\widehat{\omega_{D,6}^2}} \tag{29}$$

is clearly a biased estimator for ω_D. To make a fair comparison between $\hat{\omega}_{D,5}$ in (21) and $\hat{\omega}_{D,6}$, we use the same first-order Taylor expansion approximation, which yields

$$E[\hat{\omega}_{D,6}] \approx \omega_D. \tag{30}$$

Eq. (28) was first proposed and substantially analyzed in [14], to estimate the spectral moment of a real Gaussian process. However, the envelope-squared non-Gaussian process is not considered in [14]. Furthermore, some of the conclusions made in [14] do not apply to the non-absolutely integrable correlation $J_0(\omega_D\tau)$. In addition, application of (28) to the envelope was first proposed in [19], without any statistical analysis. On the other hand, the estimators proposed in [4] and [20] can be considered as the discrete-time equivalent of (28), where integration is replaced by summation and $\dot{y}(t)$ is approximated by the first-order difference $[y((\ell+1)T_s) - y(\ell T_s)]/T_s$, with $\ell = 0, 1, ...$, and T_s as the sampling period.

IV. Analytic Performance Analysis

In this section we provide closed-form expressions for the variance of the inphase-based estimators discussed in the previous section. This has been possible due to the Gaussianity of $\xi(t)$. For the non-Gaussian envelope-squared process $\eta(t)$, it is very difficult, if not impossible, to derive closed-from results, and Monte Carlo simulation is the only resort. Throughout this section we consider an arbitrary PDF for the AOA in (3), which makes the results of this section applicable to any possible $r_h(\tau)$, and consequently, $r_\xi(\tau)$.

In what follows, we derive closed-form expressions for the variance of $\xi(t)$-based estimators $\hat{\omega}_{D,1}$, $\hat{\omega}_{D,2}$, $\hat{\omega}_{D,5}$, and $\hat{\omega}_{D,6}$. Then we show that as the observation time T increases, the variances of all these estimators converge to zero at the same rate of $\ln(T)/T$, where $\ln(.)$ is the natural logarithm. This novel result shows the asymptotic equivalence of these four estimators.

A. Crossing-Based Methods

For a zero-mean, unit-variance, and real Gaussian $\zeta(t)$, the following result is given in [14] for the variance of $(2\pi/T)N_\zeta(0,T)$, the normalized number of zero upcrossings of $\zeta(t)$ over $(0,T]$

$$Var[\frac{2\pi}{T}N_\zeta(0,T)] = \frac{2\pi\gamma}{T} + \frac{2}{T}\int_0^T \Big(1-\frac{\tau}{T}\Big) \times \Bigg[\frac{\sigma_\zeta^2(\tau)}{\sqrt{1-r_\zeta^2(\tau)}}\Big\{\sqrt{1-\rho_\zeta^2(\tau)} + \rho_\zeta(\tau)\cos^{-1}(-\rho_\zeta(\tau))\Big\} - \gamma^2\Bigg] d\tau, \tag{31}$$

where $r_\zeta(\tau) = E[\zeta(t)\zeta(t+\tau)]$ and

$$\begin{aligned} \gamma^2 &= -r_\zeta''(0), \\ \sigma_\zeta^2(\tau) &= \gamma^2 - r_\zeta'^2(\tau)/[1-r_\zeta^2(\tau)], \\ \rho_\zeta(\tau) &= -r_\zeta''^2(\tau) - r_\zeta(\tau)r_\zeta'^2(\tau)/[1-r_\zeta^2(\tau)]. \end{aligned} \tag{32}$$

With $\zeta(t) = \sqrt{2}\xi(t)$, variance of $\hat{\omega}_{D,1}$ in (11) can be easily expressed in terms of (31). To calculate the variance of $\hat{\omega}_{D,2}$ in (12) using (31), we note that each maximum of $\xi(t)$ corresponds to a zero downcrossing of the derivative $\dot{\xi}(t)$. Since the number of zero upcrossings and downcrossings are the same, we conclude that $M_\xi(T) = N_{\dot{\xi}}(0,T)$. This, along with $\zeta(t) = (2/\omega_D)\dot{\xi}(t)$ and $r_{\dot{\xi}}(\tau) = -r_\xi''(\tau)$, gives the variance of $\hat{\omega}_{D,2}$ in closed from.

By extending the asymptotic analysis of [14] to our estimators, and using the asymptotic form of $r_h(\tau)$ [21]

$$r_h(\tau) = \Big(\frac{\omega_D\tau}{2\pi}\Big)^{-1/2}[p_h(0)e^{j(\omega_D\tau-\pi/4)} + p_h(\pi)e^{-j(\omega_D\tau-\pi/4)}] + O(\tau^{-1}),\ \text{as } \tau\to\infty, \tag{33}$$

in Appendix II we have proved

$$Var[\hat{\omega}_{D,1}], Var[\hat{\omega}_{D,2}] = O(T^{-1}\ln T),\ \text{as } T\to\infty. \tag{34}$$

This interesting new result shows that for large observation intervals, the variance of both estimators converges to zero at the same rate.

B. Covariance-Based Methods

1) Covariance matching method: Based on the fourth-order moment of zero-mean and jointly Gaussian variables [22], and using the definition of the covariance estimator given in (22), it can be shown that

$$E[\hat{c}_\xi(\tau_1)\hat{c}_\xi(\tau_2)] = c_\xi(\tau_1)c_\xi(\tau_2) + \frac{1}{T}\int_{-T}^{T}\left(1-\frac{|\tau|}{T}\right) \times [c_\xi(\tau)c_\xi(\tau+\tau_2-\tau_1) + c_\xi(\tau+\tau_2)c_\xi(\tau-\tau_1)]d\tau. \quad (35)$$

For $\tau_1 = \tau_2$, (35) simplifies to eq. (5.69) given in [23, p. 194]. Using (23), it is straightforward to calculate the variance of $\widehat{\omega_{D,5}^2}$, defined in (20)

$$Var[\widehat{\omega_{D,5}^2}] = \left(\frac{5}{bT_0^5}\right)^2 \int_0^{T_0}\int_0^{T_0} \tau_1^2\tau_2^2\{E[\hat{c}_\xi(\tau_1)\hat{c}_\xi(\tau_2)] - c_\xi(\tau_1)c_\xi(\tau_2)\}d\tau_1 d\tau_2. \quad (36)$$

As before, we consider the first-order Taylor expansion [14] for $\sqrt{\widehat{\omega_{D,5}^2}}$ around $E[\widehat{\omega_{D,5}^2}] = \omega_D^2$, which implies that

$$Var[\hat{\omega}_{D,5}] \approx Var[\widehat{\omega_{D,5}^2}]/(4E[\widehat{\omega_{D,5}^2}]), \quad (37)$$

with the numerator and denominator given in (36) and (23), respectively.

If T_0 is small enough, we can assume $\hat{\omega}_{D,5}$ is approximately unbiased, as shown in (25), and therefore $Var[\hat{\omega}_{D,5}]$ in (37) is enough to assess the performance. However, if the bias is not negligible, we need to look at the estimation error $E[(\hat{\omega}_{D,5}-\omega_D)^2] = Var[\hat{\omega}_{D,5}]+(E[\hat{\omega}_{D,5}]-\omega_D)^2$. With $T = 1$ sec. and uniform PDF for the AOA, i.e., $c_\xi(\tau)$ given by (15), the estimation error of $\hat{\omega}_{D,5}/(2\pi)$ is plotted in Fig. 1 versus T_0. COV in the legend box is the abbreviation for covariance and the subscript T stands for theoretical. Note that for each f_D, there is a single $T_{0,opt}$ which yields the smallest estimation error. For $T_0 < T_{0,opt}$, the estimation error could be very large, specially for small f_D s. On the other hand, for each f_D, there is a neighborhood around $T_{0,opt}$, over which the estimation error remains almost constant. As f_D increases, this neighborhood becomes smaller.

At this point, it seems difficult to study the asymptotic performance of $\hat{\omega}_{D,5}$, due to the complicated form of the estimator's bias, variance, and the parameter T_0 involved. However, the indirect argument of [21, p. 2204, the paragraph right before the Conclusions], which takes

advantage of the asymptotic properties of moment-based estimators, without deriving the variance expressions explicitly, might be applicable, which yields $Var[\hat{\omega}_{D,5}] \approx O(T^{-1}\ln T)$, as $T \to \infty$.

2) Integration method: Based on in [14, eq. (2.1)], the variance of $\widehat{\omega_{D,6}^2}$ in (28) can be written as

$$Var[\widehat{\omega_{D,6}^2}] = \frac{64}{T}\int_0^T \left(1-\frac{\tau}{T}\right) r_\xi''^2(\tau)d\tau. \tag{38}$$

Again we consider the first-order Taylor expansion [14] for $\sqrt{\widehat{\omega_{D,6}^2}}$ around $E[\widehat{\omega_{D,6}^2}] = \omega_D^2$, i.e., $Var[\hat{\omega}_{D,6}] \approx Var[\widehat{\omega_{D,6}^2}]/(4E[\widehat{\omega_{D,6}^2}])$. Therefore

$$Var[\hat{\omega}_{D,6}] \approx \frac{16}{\omega_D^2 T}\int_0^T \left(1-\frac{\tau}{T}\right) r_\xi''^2(\tau)d\tau. \tag{39}$$

There are two integrals on the right-hand side of (39). Based on the asymptotic form of $r_\xi''^2$ in (57), Appendix II, and by integrating τ^{-1}, the first integral yields $O(\ln T), T \to \infty$. Using a similar argument, the second integral can be easily shown to be $O(T), T \to \infty$. Therefore $TVar[\hat{\omega}_{D,6}] \approx O(\ln T) + T^{-1}O(T) = O(\ln T)$, as $T \to \infty$. So the asymptotic variance of $\hat{\omega}_{D,6}$ can be written as

$$Var[\hat{\omega}_{D,6}] \approx O(T^{-1}\ln T), \text{ as } T \to \infty. \tag{40}$$

Interestingly, the Holtzman-Sampath estimator given in eq. (10) of [21] is the discrete-time equivalent of $\hat{\omega}_{D,6}$ in (29). Our asymptotic result in (40) agrees with the asymptotic variance given in the last two lines of Sec. 4 of [21], p. 2204, obtained via a different approach and in a discrete-time setting.

V. Simulation Results and Performance Comparison

In this section we consider four inphase-based and four envelope-based estimators and compare their performance in terms of the estimation error, which is defined to be the root mean square error (RMSE), given by

$$\left(E[(\hat{\omega}_{D,i}-\omega_D)^2]\right)^{\frac{1}{2}} = \left(Var[\hat{\omega}_{D,i}] + (E[\hat{\omega}_{D,i}]-\omega_D)^2\right)^{\frac{1}{2}}, \tag{41}$$

where $i = 1, 2, ..., 8$, and the second term in the right side stands for the bias. Rayleigh fading channel is first considered to investigate the estimation error of all these estimators. For the inphase-based methods we have used the closed-form expressions (31), (36) and (39) to calculate the variance, whereas the bias is computed using (44), (45), (46) and (47) in Appendix I. The

estimation errors of the envelope-based techniques for Rayleigh channel are obtained via Monte Carlo simulation. On the other hand, for Rician fading, the estimation errors of both the inphase-based and envelope-based estimators are evaluated, through Monte Carlo simulations. Using the spectral method [24], 100 independent realizations of complex Gaussian processes are generated, with $N = 10000$ complex samples per realization, which is equivalent to $T = 1$ sec. The simulated autocorrelations are given in (6) and (4) for Rayleigh and Rician fading, respectively. The spectral method is also used for generating the lowpass complex Gaussian bandlimited noise, with a flat power spectrum over the fixed receiver bandwidth of $B = 101$ Hz. This allows for estimating the maximum Doppler frequency up to 101 Hz. By increasing B, higher f_Ds can be estimated. In simulations, we look at the estimation error of eight estimators $\hat{f}_D = \hat{\omega}_D/(2\pi)$. The abbreviations LCR, ROM, INT, COV, and ZCR in legend boxes refer to the level crossing rate, rate of maxima, integration, covariance, and zero crossing rate, respectively. In addition, the subscripts S and T stand for simulated and theoretical, respectively.

Note that in the covariance matching method, using either the inphase component or the envelope, we need to specify T_0. Since $T_{0,opt}$ varies over a large range, as f_D changes, in the sequel, unless specified otherwise, we choose $T_0 = 0.005$ and 0.06 sec., from Fig. 1, for $31 \leq f_D \leq 81$ and $1 \leq f_D < 31$ Hz, respectively. This means that we are assuming a rough prior knowledge on the speed is available, when using the covariance matching method. Also note that choosing the appropriate T_0 for the envelope-based covariance matching, from the inphase-based curves of Fig. 1, is convenient but not optimum. Clearly, there is no need to predetermine any parameter for the other six methods.

We first validate our performance analysis for the four inphase-based estimators, via Monte-Carlo simulation. As shown in Fig. 2, where noise-free isotropic scattering is considered, the derived theoretical estimation error expressions are in good agreement with simulation. Note that for the covariance matching method appropriate $T_{0,opt}$ is chosen from Fig. 1 for each f_D, to only compare the simulation and theory.

Based on Fig. 3, where we have isotropic scattering without noise, InphaseROM and EnvelopeROM demonstrate the best performance, whereas InphaseCOV and EnvelopeCOV are the worst. When including the effect of nonisotropic scattering without noise, depicted in Fig. 4, InphaseROM is the best and Envelope{LCR, INT, COV} are the worst for $f_D \geq 10$ Hz, whereas InphaseCOV shows large errors when $f_D < 10$ Hz. The effect of the nonisotropic scattering

parameter κ is shown in Fig. 5, where $\alpha = 0^{\text{o}}$ and $f_D = 21$. One can see that Inphase{ROM, COV} are robust against κ. Fig. 6 illustrates the estimation error versus the mean AOA α, for $\kappa = 3.3$ [13] and $f_D = 21$ Hz. Once again, InphaseROM demonstrates a robust performance. Note that the optimal $T_0 = 0.02$ sec. is chosen from Fig. 1, for $f_D = 21$ Hz, and used in both Fig. 5 and Fig. 6.

Fig. 7 and Fig. 8 demonstrate the effect of the LOS parameters K and ϕ_0 in a noise-free isotropic fading channel with $f_D = 21$ Hz, respectively. As one can see in Fig. 7, ROM-based and COV-based methods are fairly insensitive to the Rice factor K, with ROM-based methods showing much smaller errors. In terms of the robustness to the LOS AOA ϕ_0 in Fig. 8, COV-based estimators are less sensitive, whereas the InphaseZCR estimation error change significantly.

With isotropic scattering and a finite SNR of 10 dB, Fig. 9 shows the impact of noise. For large Dopplers, all the techniques do reasonably well in the presence of noise. One could also say that for medium and large Dopplers, $f_D \geq 20$ Hz, InphaseZCR is the best choice. On the other hand, when f_D is small, InphaseCOV and EnvelopeCOV perform better than the other techniques. This is due to the proper choice of the parameter T_0 for small speeds.

Finally we investigate the effect of the estimation time window T. Fig. 10 shows the estimation error with respect to T, for a noiseless isotropic Rayleigh fading channel with $f_D = 21$ Hz. Clearly all the crossing-based techniques degrade for very short observation intervals, say, $T < 25$ msec. This is also observed in [6] and the reason is that the channel does not experience many crossings in a short time interval. Overall, for $T > 50$ msec, all the eight estimators are approximately insensitive to the choice of T.

VI. Conclusion

In this paper we have studied a variety of crossing-based and covariance-based speed estimation techniques, in a unified framework. Such a framework has helped us to assess the performance of all the estimators, analytically, under the same umbrella, when the inphase component is used. As a by-product of this approach, we have demonstrated, mathematically, that for large observation intervals, the performance of all these estimators is the same. Closed-form expressions for the bias and variance of the inphase-based estimators are also derived and verified via simulation. We have observed that when noise is negligible, rate of maxima of the inphase component and also the envelope provide the best performance. The proposed rate of maxima

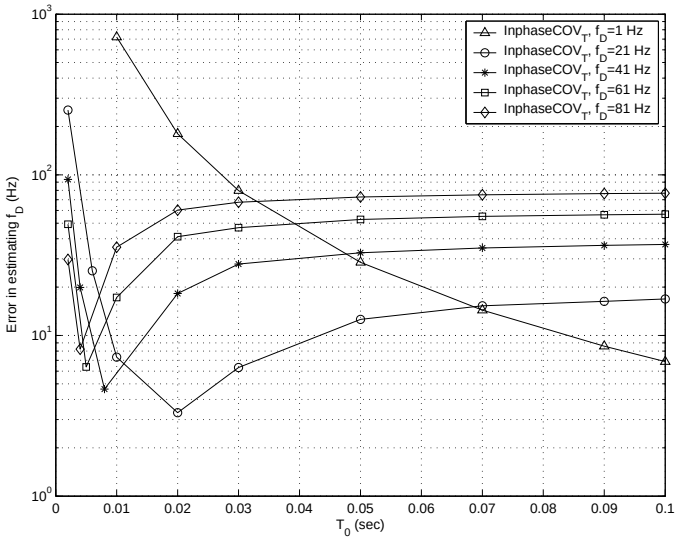

Fig. 1. Estimation error of the covariance matching method using the inphase component, versus the parameter T_0, assuming isotropic scattering.

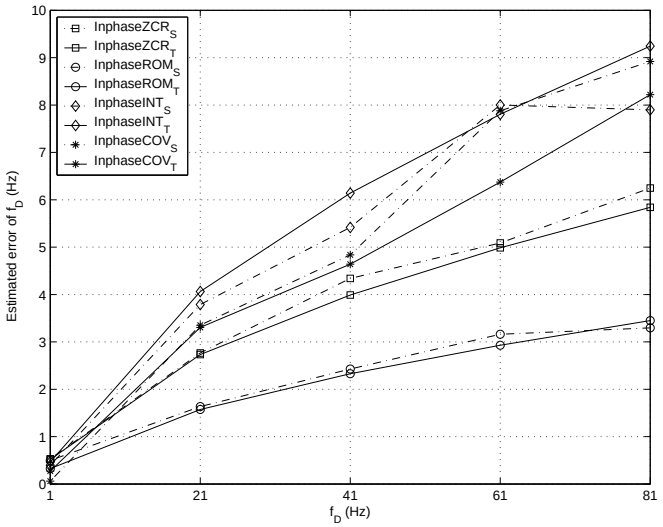

Fig. 2. Comparison of simulated and theoretical estimation errors for four inphase-based estimators, versus the maximum Doppler frequency (no noise, isotropic scattering).

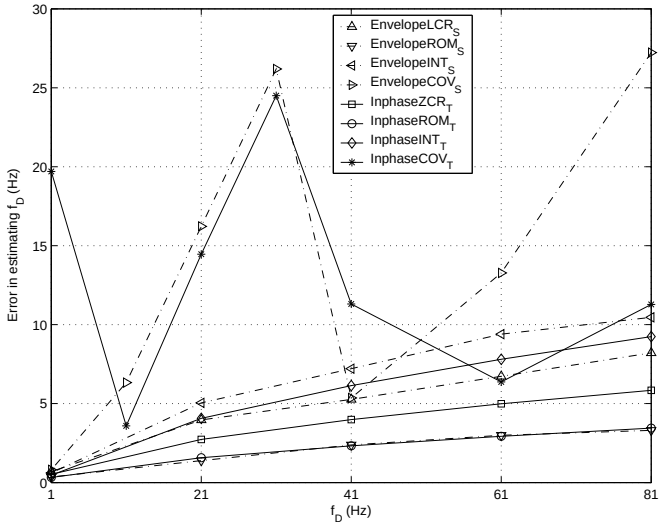

Fig. 3. Estimation errors of eight estimators versus the maximum Doppler frequency (no noise, isotropic scattering).

of the inphase component also remains to be the best with respect to the nonisotropic scattering parameter and Ricean factor. When noise is not negligible and speed is high, most of the methods show a good performance. In particular, for medium and high speeds, the zero crossing rate of the inphase component is the best choice. However, for small speeds, the covariance matching technique seems to be capable of providing an accurate estimate, when noise is present, provided that the parameter T_0 is chosen properly. For very small observation intervals, covariance-based estimators demonstrate a better performance.

APPENDIX I
EXPECTED VALUES OF THE INPHASE-BASED ESTIMATORS IN NOISY RAYLEIGH CHANNELS WITH NONISOTROPIC SCATTERING

All the speed estimators discussed in this paper are unbiased or approximately unbiased, only under the assumption of a noise-free isotropic Rayleigh fading channel, where $r_h(\tau) = J_0(\omega_D \tau)$. To evaluate the theoretical estimation errors of the inphase-based speed estimators in (11), (12), (21) and (29), in a noisy nonisotropic Rayleigh fading channel, we have the following correlation function for the received signal $z(t)$, according to (1) and (4)

$$r_z(\tau) = r_x(\tau) + r_n(\tau) = \Omega r_h(\tau) + r_n(\tau). \tag{42}$$

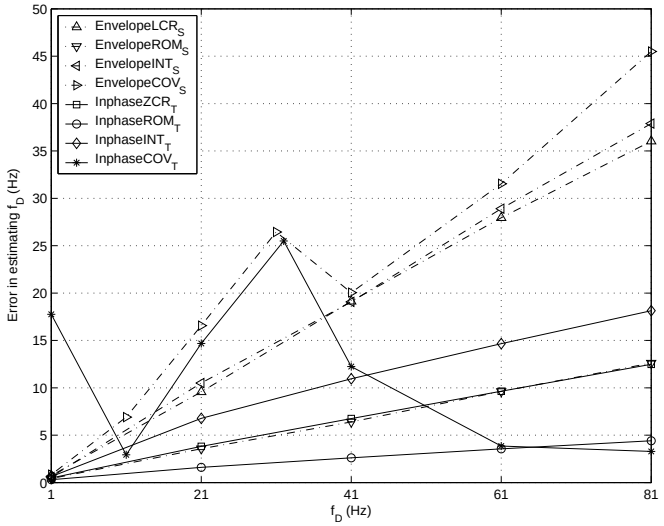

Fig. 4. Estimation errors of eight estimators versus the maximum Doppler frequency (no noise, nonisotropic scattering).

For $r_h(\tau)$ in (42) we use (6), whereas the noise correlation function $r_n(\tau) = E[n(t)n^*(t+\tau)]$ is given by $\Omega_n \sin(2\pi B\tau)/(2\pi B\tau)$. This corresponds to a bandlimited flat-spectrum lowpass complex noise with the power Ω_n and the bandwidth B in Hz. The SNR is defined as Ω/Ω_n, and $\Omega = 1$ is assumed, without loss of generality. As mentioned previously, $B = 101$ Hz is used throughout the simulations. Note that the variance expressions in (31), (37) and (39) hold for (42) in general. This is simply because in Rayleigh fading, $z(t)$ in (1) is still a zero-mean Gaussian process, irrespective of the fading correlation and as long as the additive noise is zero-mean and Gaussian. So, equations (31), (37) and (39) which hold for a real zero-mean Gaussian process with an arbitrary correlation function, can be also used for the real part of $z(t)$, i.e., the inphase component. The correlation function for $z(t)$ is given in (42), derived under the reasonable assumption of independent channel and noise. Closed-form formulas for the expected value of the four inphase-based estimators are given in the sequel. They hold for (42) as well.

Let us define $\beta(t) = \Re\{z(t)\}$, with $z(t)$ given in (1). For $r_\beta(\tau) = E[\beta(t)\beta^*(t+\tau)]$, we have $r_\beta(\tau) = (1/2)\Re\{r_z(\tau)\}$. It is well known that the zero crossing rate of a real Gaussian process can be calculated using its correlation function [1], which for $\beta(t)$ and using (42), can be written

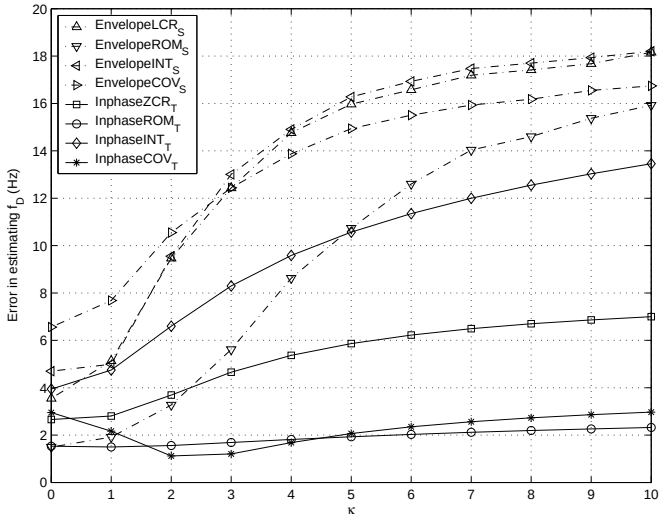

Fig. 5. Estimation errors of eight estimators versus κ, $f_D = 21$ Hz, $\alpha = 0^{\rm o}$ (no noise, nonisotropic scattering).

as

$$\frac{E[N_\beta(0,T)]}{T} = \frac{1}{2\pi}\sqrt{\frac{-r''_\beta(0)}{r_\beta(0)}}$$
$$= \frac{1}{2\pi}\sqrt{\frac{4\pi^2 B^2 \Omega_n}{3(1+\Omega_n)} + \frac{\omega_D^2(I_0(\kappa)+I_2(\kappa)\cos(2\alpha)}{2(1+\Omega_n)I_0(\kappa)}}. \tag{43}$$

By replacing $N_\xi(0,T)$ in (11) with $N_\beta(0,T)$, the mean of the InphaseZCR estimator can be written as

$$E[\hat{\omega}_{D,1}] = \sqrt{\frac{8\pi^2 B^2 \Omega_n}{3(1+\Omega_n)} + \frac{\omega_D^2(I_0(\kappa)+I_2(\kappa)\cos(2\alpha))}{(1+\Omega_n)I_0(\kappa)}}. \tag{44}$$

For $\Omega_n = \kappa = 0$, i.e., noise-free isotropic scattering, (44) reduces to $E[\hat{\omega}_{D,1}] = \omega_D$, as mentioned right after (14).

As mentioned before, the number of maxima of a process is the same as the number of upward or downward zero crossings of the derivative of the process. Therefore the rate of maxima of $\beta(t)$ can be calculated based on $\dot{\beta}(t)$ as

$$\frac{E[M_\beta(T)]}{T} = \frac{1}{2\pi}\sqrt{\frac{-r''_{\dot\beta}(0)}{r_{\dot\beta}(0)}} = \frac{1}{2\pi}\sqrt{\frac{r^{(4)}_\beta(0)}{-r''_\beta(0)}}. \tag{45}$$

where $r^{(4)}_\beta(\tau)$ is the fourth derivative with respect to τ. The lengthy closed form of (45) is not given to save space. By replacing $M_\xi(T)$ in (12) with $M_\beta(T)$, the mean of the InphaseROM

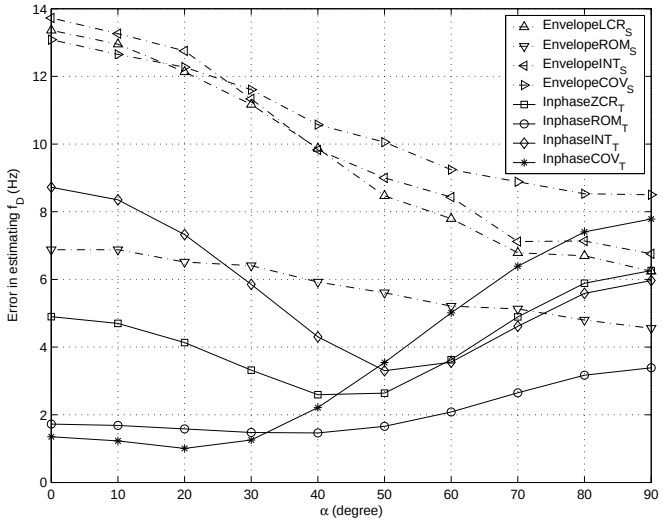

Fig. 6. Estimation errors of eight estimators versus α, $f_D = 21$ Hz, $\kappa = 3.3$ (no noise, nonisotropic scattering).

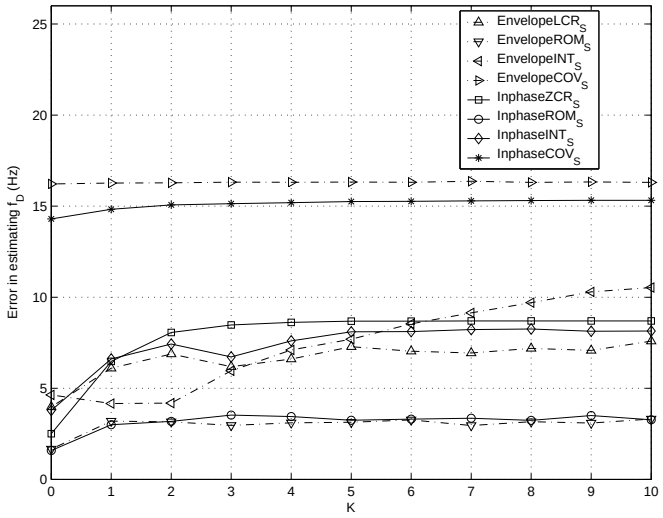

Fig. 7. Estimation errors of eight estimators versus K, $f_D = 21$ Hz, $\phi_0 = 0^{\text{o}}$ (no noise, isotropic scattering).

estimator can be easily derived, using (45). For isotropic Rayleigh fading without noise and $\Omega = 1$, we get $r_z(\tau) = J_0(\omega_D \tau)$ from (42). This makes it easy to verify that $E[\hat{\omega}_{D,2}] = \omega_D$, as mentioned right after (14).

To calculate the expected value of the InphaseCOV estimator in (21), we use the approximation $E[\hat{\omega}_{D,5}] \approx \sqrt{E[\widehat{\omega^2_{D,5}}]}$ introduced previously. The term under the square root can be calculated from (23), where $c_y(\tau)$ is replaced by $c_\beta(\tau) = r_\beta(\tau) - \{E[\beta(t)]\}^2 = r_\beta(\tau) = (1/2)\Re\{r_z(\tau)\}$,

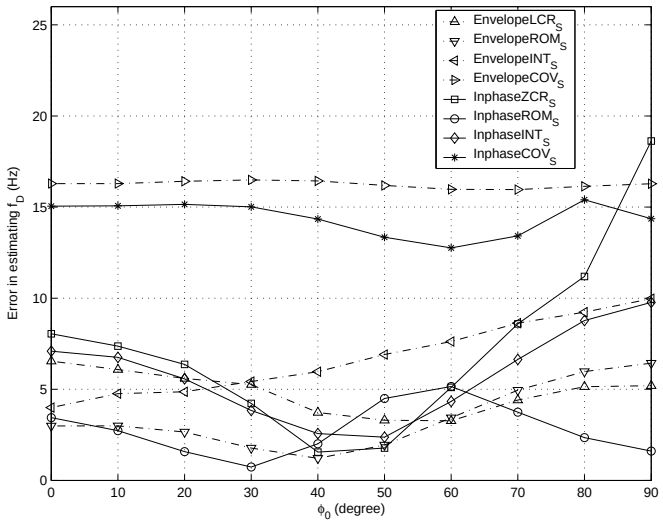

Fig. 8. Estimation errors of eight estimators versus ϕ_0, $f_D = 21$ Hz, $K = 2$ (no noise, isotropic scattering).

$a = 1/2$ and $b = 1/8$. Note that $r_z(\tau)$ is given in (42). This gives the expected value of the inphaseCOV estimator as

$$E[\hat{\omega}_{D,5}] = \sqrt{\frac{20}{3T_0^2} - \frac{40}{T_0^5}\int_0^{T_0} \tau^2 r_\beta(\tau) d\tau}. \tag{46}$$

To obtain the expected value of the InphaseINT estimator in (29), we use the approximation $E[\hat{\omega}_{D,6}] \approx \sqrt{E[\widehat{\omega_{D,6}^2}]}$. The term under the square root can be calculated from (28), with $d = 4$ and $y(t)$ replaced by $\beta(t)$. Since $E[\dot{\beta}^2(t)] = r_{\dot{\beta}}(0) = -r''_\beta(0)$ and $r_\beta(\tau) = (1/2)\Re\{r_z(\tau)\}$, with $r_z(\tau)$ given in (42), one can easily show

$$\begin{aligned} E[\hat{\omega}_{D,6}] &\approx \sqrt{-4r''_\beta(0)} \\ &= \sqrt{\frac{8\pi^2 B^2 \Omega_n}{3} + \frac{\omega_D^2 (I_0(\kappa) + I_2(\kappa)\cos(2\alpha))}{I_0(\kappa)}}. \end{aligned} \tag{47}$$

For $\Omega_n = \kappa = 0$, i.e., noise-free isotropic scattering, (47) simplifies to $E[\hat{\omega}_{D,6}] \approx \omega_D$, as given in (30).

APPENDIX II
THE ASYMPTOTIC VARIANCE OF THE INPAHSE-BASED CROSSING ESTIMATORS

Here we prove the asymptotic results given in (34). According to (3.10) in [14], that part of the integrand in (31) which is within the square brackets can be written as

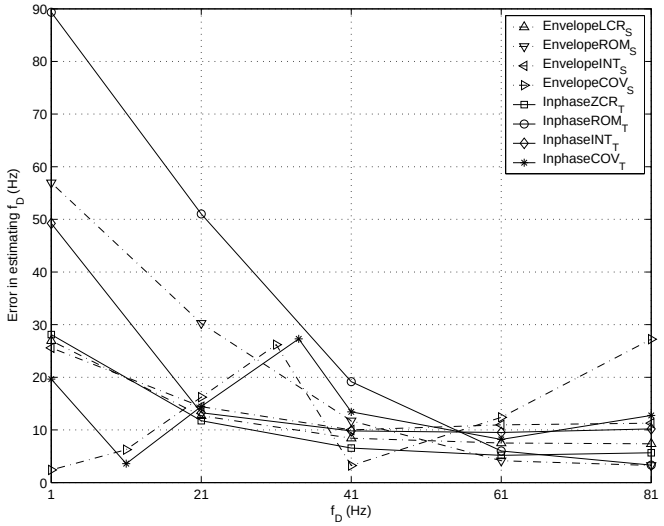

Fig. 9. Estimation errors of eight estimators versus the maximum Doppler frequency (SNR=10 dB, isotropic scattering).

$$\frac{\sigma_\zeta^2(\tau)}{\sqrt{1-r_\zeta^2(\tau)}}\left\{\sqrt{1-\rho_\zeta^2(\tau)}+\rho_\zeta(\tau)\cos^{-1}(-\rho_\zeta(\tau))\right\}-\gamma^2$$
$$=\frac{1}{2}\pi\left\{-r_\zeta''(\tau)+O\left[r_\zeta^2(\tau)+r_\zeta'^2(\tau)+r_\zeta''^2(\tau)\right]\right\},\ \text{as } \tau\to\infty. \tag{48}$$

To derive the asymptotic performance of $\hat{\omega}_{D,1}$ in (11), we note that with $\zeta(t)=\sqrt{2}\xi(t)$ we have $r_\zeta(\tau)=2r_\xi(\tau)=\Re\{r_h(\tau)\}$. Based on (33), it can be easily shown that

$$r_\xi(\tau)=\frac{\omega_D^{-1/2}\sqrt{2\pi}g}{2}\tau^{-1/2}\cos(\omega_D\tau-\pi/4)+O(\tau^{-1}),\ \text{as } \tau\to\infty, \tag{49}$$

where $g=p_h(0)+p_h(\pi)$. Also since $\tau^{-1}\cos^2(\omega_D\tau-\pi/4)=(\tau^{-1}/2)+(\tau^{-1}/2)\cos(2\omega_D\tau-\pi/2)=\tau^{-1}/2+O(\tau^{-1})$, as $\tau\to\infty$, we get

$$r_\xi^2(\tau)=\frac{\omega_D^{-1}\pi g^2}{4}\tau^{-1}+O(\tau^{-1}),\ \text{as } \tau\to\infty. \tag{50}$$

By taking the derivative of (3) we obtain

$$r_h'(\tau)=\int_{-\pi}^{\pi}-j\omega_D\cos(\phi)p_h(\phi)\exp[-j\omega_D\cos(\phi)\tau]d\phi. \tag{51}$$

Since the only difference between (51) and $r_h(\tau)$ in (3) is the extra term $-j\omega_D\cos(\phi)$, the following asymptotic form can be derived for $r_h'(\tau)$, by replacing $p_h(\phi)$ in (33) with $-j\omega_D p_h(\phi)\cos\phi$

$$r_h'(\tau)=-j\omega_D\left(\frac{\omega_D\tau}{2\pi}\right)^{-1/2}\left[p_h(0)e^{j(\omega_D\tau-\pi/4)}-p_h(\pi)e^{-j(\omega_D\tau-\pi/4)}\right]+O(\tau^{-1}),\ \text{as } \tau\to\infty. \tag{52}$$

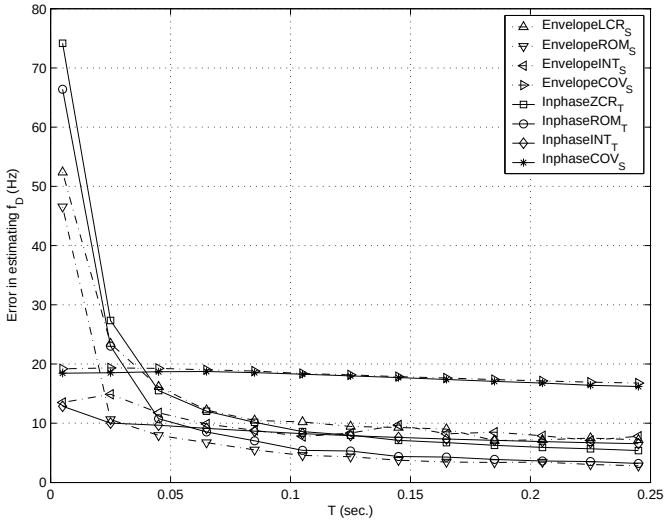

Fig. 10. Estimation errors of eight estimators versus T, $f_D = 21$ Hz, $K = 0$ (no noise, isotropic scattering).

Following the same procedure further results in

$$r_h''(\tau) = -\omega_D^2 \left(\frac{\omega_D \tau}{2\pi}\right)^{-1/2} \left[p_h(0) e^{j(\omega_D \tau - \pi/4)} + p_h(\pi) e^{-j(\omega_D \tau - \pi/4)}\right] + O(\tau^{-1}), \text{ as } \tau \to \infty. \quad (53)$$

Since $r_\xi(\tau) = (1/2)\Re\{r_h(\tau)\}$, by taking the real parts of (52) and (53), we easily obtain

$$r_\xi'(\tau) = \frac{\sqrt{2\pi\omega_D} g}{2} \tau^{-1/2} \sin(\omega_D \tau - \pi/4) + O(\tau^{-1}), \text{ as } \tau \to \infty, \quad (54)$$

$$r_\xi''(\tau) = -\frac{\omega_D^{3/2}\sqrt{2\pi} g}{2} \tau^{-1/2} \cos(\omega_D \tau - \pi/4) + O(\tau^{-1}), \text{ as } \tau \to \infty. \quad (55)$$

Also since the asymptotic form for both $\tau^{-1}\sin^2(\omega_D\tau - \pi/4)$ and $\tau^{-1}\cos^2(\omega_D\tau - \pi/4)$ is $\tau^{-1}/2 + O(\tau^{-1})$, we further obtain

$$r_\xi'^2(\tau) = \frac{\pi g^2 \omega_D}{4} \tau^{-1} + O(\tau^{-1}), \text{ as } \tau \to \infty, \quad (56)$$

$$r_\xi''^2(\tau) = \frac{\pi g^2 \omega_D^3}{4} \tau^{-1} + O(\tau^{-1}), \text{ as } \tau \to \infty. \quad (57)$$

Based on $r_\zeta(\tau) = 2r_\xi(\tau)$ and after replacing $r_\zeta^2(\tau)$, $r_\zeta'^2(\tau)$, and $r_\zeta''^2(\tau)$ in (48) with (50), (56) and (57), respectively, the right-hand side of (48) simplifies to

$$-\pi r_\xi''(\tau) + O(\tau^{-1}), \text{ as } \tau \to \infty. \quad (58)$$

As becomes clear soon, the following two results are needed to calculate the asymptotic variance of $\hat{\omega}_{D,1}$

$$\int_0^T r''_\xi(\tau)d\tau = r'_\xi(T) - r'_\xi(0) = \frac{\sqrt{2\pi\omega_D}g}{2}T^{-1/2}\sin(\omega_D T - \pi/4) + O(T^{-1}) \\ = O(T^{-1/2}),\ \text{as } T \to \infty, \tag{59}$$

$$\int_0^T \tau r''_\xi(\tau)d\tau = Tr'_\xi(T) - r'_\xi(T) + r'_\xi(0) = \frac{\sqrt{2\pi\omega_D}g}{2}T^{1/2}\sin(\omega_D T - \pi/4) + O(1) \\ + \frac{\sqrt{2\pi}\omega_D^{-1/2}g}{2}T^{-1/2}\cos(\omega_D T - \pi/4) + O(T^{-1}) \\ = O(T^{1/2}),\ \text{as } T \to \infty. \tag{60}$$

Note that $r'_\xi(T)$ and $r_\xi(T)$ for large T are obtained from (54) and (49), respectively.

There are two integrals on the right-hand side of (31). By replacing the whole square brackets in (31) with (58), the first integral can be shown to be $O(T^{-1/2}) + O(\ln T)$, as $T \to \infty$. The former term is coming from (59), whereas the latter is the integral of τ^{-1}. Furthermore, by replacing the whole square brackets in (31) with (58), the second integral can be reduced to $O(T^{1/2}) + O(T)$, as $T \to \infty$. The former is taken from (60) and the latter is the integral of 1. Therefore, the whole integral on the right-hand side of (31) can be written as $O(T^{-1/2}) + O(\ln T) + T^{-1}[O(T^{1/2}) + O(T)] = O(\ln T)$, as $T \to \infty$. This completes the proof of (34) for the asymptotic variance of $\hat{\omega}_{D,1}$.

To prove the asymptotic performance of the estimator in (12), first note that now $\zeta(t) = (2/\omega_D)\dot{\xi}(t)$. Therefore $r_\zeta(\tau)$ in (48) is given by

$$r_\zeta(\tau) = (4/\omega_D^2)r_{\dot{\xi}}(\tau) = -(4/\omega_D^2)r''_\xi(\tau) = -(2/\omega_D^2)\Re\{r''_h(\tau)\}, \tag{61}$$

where $r''_h(\tau)$ is given by (53). Obviously, we have $r'_\zeta(\tau) = -(2/\omega_D^2)\Re\{r_h^{(3)}(\tau)\}$ and $r''_\zeta(\tau) = -(2/\omega_D^2)\Re\{r_h^{(4)}(\tau)\}$, where $r_h^{(3)}(\tau)$ and $r_h^{(4)}(\tau)$ asymptotically behave as follows

$$r_h^{(3)}(\tau) = j\omega_D^3\left(\frac{\omega_D\tau}{2\pi}\right)^{-1/2}\left[p_h(0)e^{j(\omega_D\tau-\pi/4)} - p_h(\pi)e^{-j(\omega_D\tau-\pi/4)}\right] + O(\tau^{-1}),\ \text{as } \tau \to \infty, \tag{62}$$

and

$$r_h^{(4)}(\tau) = \omega_D^4\left(\frac{\omega_D\tau}{2\pi}\right)^{-1/2}\left[p_h(0)e^{j(\omega_D\tau-\pi/4)} + p_h(\pi)e^{-j(\omega_D\tau-\pi/4)}\right] + O(\tau^{-1}),\ \text{as } \tau \to \infty. \tag{63}$$

These two are obtained following the same technique used to derive (52). When comparing the asymptotics of $r_h''(\tau)$ in (53) with $r_h(\tau)$ in (33), $r_h^{(3)}(\tau)$ in (62) with $r_h'(\tau)$ in (52), and $r_h^{(4)}(\tau)$ in (63) with $r_h''(\tau)$ in (53), we observe that each pair take the same form, if we ignore these constants outside the square brackets (which will not affect our conclusion). This meas that the right-hand side of (49) and then the right-hand side of (31) are asymptotically the same as those previously derived for $\hat{\omega}_{D,1}$. Therefore, the asymptotic variance of $\hat{\omega}_{D,2}$ is the same as $\hat{\omega}_{D,1}$, given in (34).

REFERENCES

[1] G. L. Stüber, *Principles of Mobile Communication*, 2nd ed. Boston, MA: Kluwer, 2001.

[2] M. J. Chu and W. E. Stark, "Effect of mobile velocity on communications in fading channels," *IEEE Trans. Veh. Technol.*, vol. 49, pp. 202–210, 2000.

[3] L. Krasny, H. Arslan, D. Koilpillai, and S. Chennakeshu, "Doppler spread estimation in mobile radio systems," *IEEE Commun. Lett.*, vol. 5, pp. 197–199, 2001.

[4] J. Holtzman and A. Sampath, "Adaptive averaging methodology for handoffs in cellular systems," *IEEE Trans. Veh. Technol.*, vol. 44, pp. 59–66, 1995.

[5] H. Zhang and A. Abdi, "Mobile speed estimation using diversity combining in fading channels," in *Proc. IEEE Global Telecommun. Conf.*, Dallas, TX, 2004, pp. 3685–3689.

[6] C. Tepedelenlioglu and G. Giannakis, "On velocity estimation and correlation properties of narrow-band mobile communication channels," *IEEE Trans. Veh. Technol.*, vol. 50, pp. 1039–1052, 2001.

[7] K. E. Baddour and N. C. Beaulieu, "Robust Doppler spread estimation in nonisotropic fading channels," *IEEE Trans. Wireless Commun.*, vol. 4, pp. 2677–2682, 2005.

[8] H. Zhang and A. Abdi, "A robust mobile speed estimator in fading channels: Performance analysis and experimental results," in *Proc. IEEE Global Telecommun. Conf.*, St. Louis, MO, 2005, pp. 2569–2573.

[9] K. Baddour and N. Beaulieu, "Nonparametric Doppler spread estimation for flat fading channels," in *IEEE Wireless Commun. and Networking Conf.*, New Orleans, LA, 2003, pp. 953–958.

[10] A. Dogandzic and B. Zhang, "Estimating Jakes' Doppler power spectrum parameters using the Whittle approximation," *IEEE Trans. Signal Processing*, vol. 53, pp. 987–1005, 2005.

[11] C. Tepedelenlioglu, A. Abdi, G. B. Giannakis, and M. Kaveh, "Estimation of Doppler spread and signal strength in mobile communications with applications to handoff and adaptive transmission," *Wirel. Commun. Mob. Comput.*, vol. 1, pp. 221–242, 2001.

[12] A. Abdi and M. Kaveh, "Parametric modeling and estimation of the spatial characteristics of a source with local scattering," in *Proc. IEEE Int. Conf. Acoust., Speech, Signal Processing*, Orlando, FL, 2002, pp. 2821–2824.

[13] A. Abdi, J. A. Barger, and M. Kaveh, "A parametric model for the distribution of the angle of arrival and the associated correlation function and power spectrum at the mobile station," *IEEE Trans. Veh. Technol.*, vol. 51, pp. 425–434, 2002.

[14] G. Lindgren, "Spectral moment estimation by means of level crossings," *Biometrika*, vol. 61, pp. 401–418, 1974.

[15] A. Abdi and S. Nader-Esfahani, "Expected number of maxima in the envelope of a spherically invariant random process," *IEEE Trans. Inform. Theory*, vol. 49, pp. 1369–1375, 2003.

[16] K. S. Miller and M. M. Rochwarger, "A covariance approach to spectral moment estimation," *IEEE Trans. Inform. Theory*, vol. 18, pp. 588–596, 1972.

[17] ——, "Some remarks on spectral moment estimation," *IEEE Trans. Commun.*, vol. 20, pp. 260–262, 1972.

[18] K. S. Miller, *Complex Stochastic Processes: An Introduction to Theory and Application*. Reading, MA: Addison-Wesley, 1974.

[19] P. A. Bello, "Some techniques for the instantaneous real-time measurement of multipath and Doppler spread," *IEEE Trans. Commun. Technol.*, vol. 13, pp. 285–292, 1965.

[20] J. M. Perl and D. Kagan, "Real-time HF channel parameter estimation," *IEEE Trans. Commun.*, vol. 34, pp. 54–58, 1986.

[21] C. Tepedelenlioglu, "Performance analysis of velocity (Doppler) estimators in mobile communications," in *Proc. IEEE Int. Conf. Acoust., Speech, Signal Processing*, Orlando, FL, 2002, pp. 2201–2204.

[22] A. Papoulis, *Probability, Random Variables, and Stochastic Processes*, 3rd ed. Singapore: McGraw-Hill, 1991.

[23] J. S. Bendat and A. G. Piersol, *Measurement and Analysis of Random Data*. New York: Wiley, 1966.

[24] K. Acolatse and A. Abdi, "Efficient simulation of space-time correlated MIMO mobile fading channels," in *Proc. IEEE Veh. Technol. Conf.*, Orlando, FL, 2003, pp. 652–656.